International Journal of Thermophysics, Vol. 16, No. 1, 1995

Holographic Grating Study of Mass and Thermal Diffusion of Polystyrene/Toluene Solutions[1]

W. Köhler,[2,3] C. Rosenauer,[2] and P. Rossmanith[2]

The transient grating technique of thermal diffusion forced Rayleigh scattering (TDFRS) has been employed to study translational and thermal diffusion of polystyrene in toluene. Different molar masses and concentrations below or slightly above the overlap concentration c^* have been investigated. The translational diffusion coefficients agree well with results obtained from photon correlation spectroscopy. Small remaining differences can be attributed to sample polydispersity. The molar mass independence of the thermal diffusion coefficient is confirmed, and thermal diffusion and Soret coefficients are compared with data obtained from thermal field flow fractionation and diffusion cell experiments.

KEY WORDS: diffusion; forced Rayleigh scattering; holography; polymer solution; thermal diffusion.

1. INTRODUCTION

The Ludwig–Soret effect, also termed thermal diffusion, of polymers in solution has attracted the interest of researchers for a long time [1–3]. Nevertheless, the understanding of the effect is still very incomplete, and frequently there is a serious disagreement in the experimental data reported by different authors.

Besides the fundamental problem of relating macroscopically observed transport coefficients to microscopic molecular properties, there is growing interest in thermal diffusion because of the molar mass dependence of the Soret coefficient, S_T, which can be utilized for polymer fractionation [4].

[1] Paper presented at the Twelfth Symposium on Thermophysical Properties, June 19–24, 1994, Boulder, Colorado, U.S.A.

[2] Max-Planck-Institut für Polymerforschung, Postfach 3148, D-55021 Mainz, Germany.

[3] To whom correspondence should be addressed.

0195-928X/95/0100-0011$07.50/0

While abundant data on the translational diffusion coefficient, D, are available, reliable data on S_T and the thermal diffusion coefficient, D_T, are scarce. Apparently, D_T is molar mass independent [5, 6], and a reliable technique for its determination from polydisperse samples is desirable, since well-characterized monodisperse samples are not available for most polymers.

Recently, thermal diffusion forced Rayleigh scattering (TDFRS) has been employed in our laboratory for the study of thermal diffusion of polymer solutions. A holographic grating is written into a slightly absorbing sample, giving rise to a thermal grating. Then, driven by thermal diffusion, a concentration grating starts to build up superimposed upon the thermal one. The combined phase grating is read by Bragg diffraction of a readout laser beam. From the time-dependent diffraction efficiency, the translational diffusion coefficient, the thermal diffusion coefficient, and the Soret coefficient are obtained in a very direct way [7, 8].

Compared to other techniques, a properly conducted heterodyne TDFRS experiment has several advantages, such as the high sensitivity of holographic detection, the minute perturbations of the sample, and the convenient subsecond lifetime of the concentration grating. Contrary to "conventional" forced Rayleigh scattering, no chemical chain labeling is required and no sample degradation is observed, which allows signal averaging over arbitrary times. Furthermore, the periodicity of the holographic grating leads to very simple solutions of the diffusion equations used for a phenomenological description.

2. THEORY

The starting point for a phenomenological description of the Ludwig–Soret effect in a binary solution is an extension of Fick's second law of diffusion [9, 10]:

$$\frac{\partial c(\vec{r}, t)}{\partial t} = D\nabla^2 c(\vec{r}, t) + D_T c(\vec{r}, t)[1 - c(\vec{r}, t)]\,\nabla^2 T(\vec{r}, t) \tag{1}$$

where c is the concentration in weight fractions, and D and D_T are the translational and the thermal diffusion coefficient, respectively, which can be related to the Onsager transport coefficients L_{mn} and L_{mq} [10]. The coupling between heat flow and concentration gradient due to the Dufour effect is neglected in Eq. (1), since it is extremely weak in solutions. Hence, the temperature distribution, $T(\vec{r}, t)$, can be determined independently from the concentration by solving the heat equation with the appropriate boundary conditions. Once $T(\vec{r}, t)$ is known, $c(\vec{r}, t)$ is obtained from Eq. (1).

Since the changes in both concentration and temperature are only very subtle, all system parameters, like the diffusion coefficients D and D_T, the thermal diffusivity, D_{th}, the density, ρ, and the specific heat, c_p, are treated as constants for a given experiment.

2.1. Writing the Grating

The two intersecting laser beams of wavelength λ_w form an optical interference grating with an intensity distribution

$$I(x, t) = I_0 + I_t(t)\, e^{iqx} \tag{2}$$

Here, polarization switching of one of the beams is assumed, which keeps the average thermal load on the sample constant. For ideal square pulse switching, I_t goes from zero to I_0.

$$q = \frac{4\pi}{\lambda_w} \sin \frac{\theta}{2} \tag{3}$$

is the absolute value of the grating vector, θ the angle of intersection, and x the coordinate perpendicular to the optical axis within the plane spanned by the two writing beams. The intensity along the optical axis is essentially constant, due to the low absorbance of the sample.

Since the fringe spacing of the grating is much smaller than the sample thickness, boundary effects are of no concern, and a one-dimensional form of the heat equation is adopted with the absorbed energy as the source term:

$$\begin{aligned} \frac{\partial T(x, t)}{\partial t} &= D_{th} \frac{\partial^2}{\partial x^2} T(x, t) + s(x, t) \\ s(x, t) &= \frac{\alpha I(x, t)}{\rho c_p} = s_0 + s_t(t)\, e^{iqx} \end{aligned} \tag{4}$$

where α is the absorption coefficient, ρ the density, and c_p the specific heat of the solution.

Equation (4) is solved by

$$\begin{aligned} T(x, t) &= T_0 + T_t(t)\, e^{iqx} \\ T_t(t) &= \int_{-\infty}^{t} dt'\, s_t(t')\, e^{-(t - t')/\tau_{th}} \end{aligned} \tag{5}$$

where $\tau_{th} = (D_{th} q^2)^{-1}$ is the lifetime and $T_t(t)$ the amplitude of the thermal grating, and T_0 the average sample temperature.

Now Eq. (1) can be solved to obtain the concentration grating caused by the Ludwig–Soret effect:

$$\begin{aligned} c(x, t) &= c_t(t)\, e^{iqx} + c_0 \\ c_t(t) &= -q^2 D_T c_0(1 - c_0) \int_{-\infty}^{t} dt'\, T_t(t')\, e^{-(t-t')/\tau} \end{aligned} \tag{6}$$

$c_t(t)$ is the amplitude and $\tau = (Dq^2)^{-1}$ the lifetime of the concentration grating. Since $c_t/c_0 < 10^{-5}$ for a typical experiment, the approximation $c(1-c) \approx c_0(1-c_0)$ holds.

For an excitation pulse $s_t(t) = s_0[h[t-t_1) - h(t-t_2)]$ lasting from t_1 to t_2, where $h(t)$ is the Heaviside step function, the amplitudes of the thermal and the concentration grating are [7, 8]

$$T_t(t) = \tau_{th} s_0[h(t-t_1)(1 - e^{-(t-t_1)/\tau_{th}}) - h(t-t_2)(1 - e^{-(t-t_2)/\tau_{th}})] \tag{7}$$

and

$$\begin{aligned} c_t(t) = &-S_T c_0(1-c_0)(s_0\tau_{th})(\tau - \tau_{th})^{-1} \\ &\times \{h(t-t_1)[\tau(1 - e^{-(t-t_1)/\tau}) - \tau_{th}(1 - e^{-(t-t_1)/\tau_{th}})] \\ &- h(t-t_2)[\tau(1 - e^{-(t-t_2)/\tau}) - \tau_{th}(1 - e^{-(t-t_2)/\tau_{th}})]\} \end{aligned} \tag{8}$$

2.2. Reading the Grating

By Bragg diffraction of a readout beam at a wavelength where the sample is transparent, the resulting refractive index grating, with contributions from both temperature and concentration, is read:

$$n(x, t) - n_0 = n_t(t)\, e^{iqx} = \left[\frac{\partial n}{\partial T} T_t(t) + \frac{\partial n}{\partial c} c_t(t) \right] e^{iqx} \tag{9}$$

where $\partial n/\partial T$ and $\partial n/\partial c$ are the respective contrast factors. Finally, the diffraction efficiencies [11] for heterodyne, η_{het}, and homodyne detection, η_{hom}, are obtained after normalization to the thermal signal:

$$\begin{aligned} \eta_{het}(t) &= (\tau_{th} s_0)^{-1} \left[T_t(t) + \frac{\partial n/\partial c}{\partial n/\partial T} c_t(t) \right] \\ \eta_{hom}(t) &= \eta_{het}^2(t) \end{aligned} \tag{10}$$

Data from monodisperse solutes, characterized by a single relaxation time, are analyzed but a fit of Eq. (10) to the measured heterodyne signal, yielding D, D_T (or $S_T = D_T/D$), and D_{th} as fit parameters.

For practical purposes, some approximations and asymptotic cases are useful. D is typically 3 to 4 orders of magnitude smaller than D_{th}, and the memory terms due to τ_{th} can safely be neglected, hence $(1-e^{-t/\tau}) \approx h(t)$.

With this approximation, D_T can be obtained from the initial slope of the normalized concentration signal, assuming $t_1 = 0$:

$$\eta_{het}(t \to 0) = 1 - tq^2 D_T c_0 (1 - c_0) \frac{\partial n/\partial c}{\partial n/\partial T} \tag{11}$$

The saturation value for long pulses is

$$\eta_{het}(t \to \infty) = 1 - S_T c_0 (1 - c_0) \frac{\partial n/\partial c}{\partial n/\partial T} \tag{12}$$

$S_T = D_T/D$ is the Soret coefficient.

3. EXPERIMENT

The experimental setup has been described in detail elsewhere [8, 12], so only the main features are discussed briefly.

The apparatus comprises a standard holographic grating setup with an argon ion laser (488 nm) for writing and a helium–neon laser (633 nm) for reading. Switching of the grating is accomplished by rotating the polarization of one of the writing beams by 90°. In the off-state, corresponding to orthogonal polarization, the sample is evenly illuminated.

The phase of the grating is controlled by a mirror mounted on a piezo crystal. The application of 180° phase jumps allows the separation of homodyne and heterodyne signal components. The local oscillator for the reference wave is simply provided by scratches on the sample cell windows. Phase drifts are compensated periodically by an active phase-tracking mechanism. Since the heterodyne signal is of a superior signal-to-noise ratio and robust against phase perturbations, whereas the homodyne is not, the heterodyne signal is used for data evaluation.

The diffracted signal is detected by means of a photomultiplier tube in photon-counting operation with a minimum sampling time of 2 μs. The optical path length of the sample cells is 0.2 mm.

Measurements have been performed on polystyrene of narrow molar mass distribution ($M_w/M_n = 1.03$–1.05) dissolved in freshly distilled toluene. The molar masses span approximately two decades ($M_w = 6.1$, 48.8, and 410 kg · mol^{-1}), and from every sample a concentration series within the dilute regime was prepared. For the 48.8- and the 410-kg · mol^{-1} samples the highest concentrations are already within the semidilute regime, if

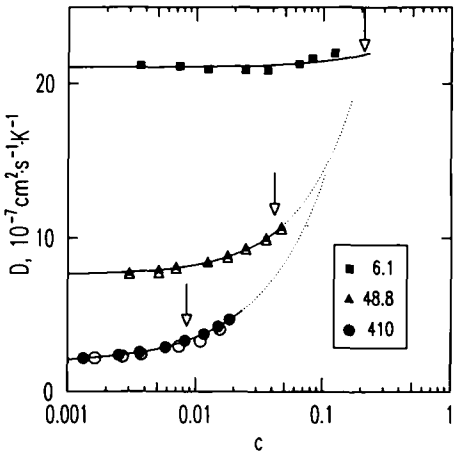

Fig. 1. Translational diffusion coefficients measured with TDFRS (filled symbols) and PCS (open symbols) of polystyrene in toluene. The PCS data are temperature corrected. Concentration as weight fraction.

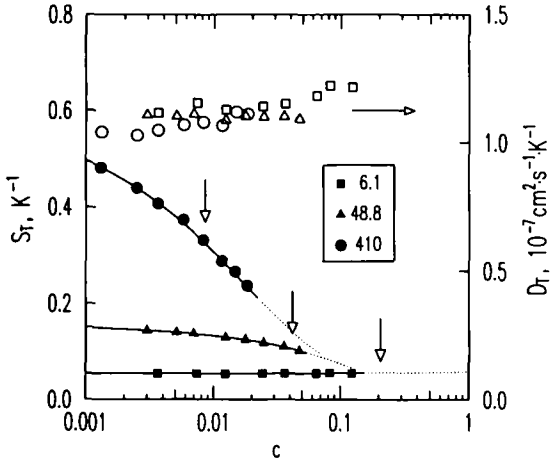

Fig. 2. Soret coefficients (filled symbols) and thermal diffusion coefficients (open symbols) of polystyrene in toluene. Concentration as weight fraction. The overlap concentrations are marked with arrows.

the overlap concentration, c^*, is taken as the reciprocal of the intrinsic viscosity: $c^* = [\eta]^{-1}$. The c^* values are marked with arrows in Figs. 1 and 2.

Quinizarin (1,4-dihydroxyanthraquinone) was added to adjust the optical density to 0.02 at a 488-nm wavelength. Typical writing intensities were 50 mW · cm $^{-2}$. All experiments were conducted at room temperature (22–24°C). The contrast factors $\partial n/\partial T$ and $\partial n/\partial c$ were measured with a scanning Michelson interferometer at a readout wavelength of 633 nm. The values found for $\partial n/\partial c$ are 0.0882 (0.103 mL · g $^{-1}$, 6.1 kg · mol $^{-1}$), 0.0924 (0.108 mL · g $^{-1}$, 48.8 kg · mol $^{-1}$), and 0.0933 (0.109 mL · g $^{-1}$, 410 kg · mol $^{-1}$), if the concentration is measured as weight fractions. The numbers in parentheses give the respective values if the concentration is measured as grams per milliliter and the molar mass of the sample. $\partial n/\partial T = -5.62 \times 10^{-4}$ K $^{-1}$ for all samples.

For the PCS experiments, a krypton ion laser (647 nm, 400 mW) and a commercial digital correlator (ALV 3000) were employed.

4. RESULTS AND DISCUSSION

It was the aim of the experiments to test the new experimental technique with well-characterized systems. Therefore most measurements were carried out below c^*, where the theoretical picture, as far as the translational diffusion coefficient is concerned, is relatively clear. There is, however, no experimental reason not to use TDFRS for semidilute or concentrated solutions, as the signal gets stronger with increasing polymer concentrations.

4.1. Translational Diffusion Coefficient

A fit of Eq. (10) to the heterodyne signals shows very little systematic deviation, which can be reduced to below the detection limit by replacing the single-exponential decay (and rise) of the concentration signal by a cumulant expansion:

$$\eta_{\text{het}}(t > t_2) \propto e^{-\Gamma(t - t_2) + 1/2\mu_2(t - t_2)^2} \tag{13}$$

$\Gamma = Dq^2 = \langle \tau^{-1} \rangle$ and $\mu_2 = \langle \tau^{-2} \rangle - \langle \tau^{-1} \rangle^2$. The averages are taken over the rate distribution function. Typical values obtained for μ_2/Γ are 0.02, and D increases by less than 1% compared to the single-exponential fit. S_T does not change noticeably. The diffusion coefficients shown in Fig. 1 are determined by a cumulant fit, and they are the correct values in the sense that they can be expressed as well-defined averages over the rate distribution functions. The polydispersity problem is revisited briefly at the end of this section.

D shows the pronounced increase with concentration—especially for the higher molar mass polymers—characteristic for the mutual diffusion of polymer and solvent within a concentration gradient of the two components. In the semidilute regime above c^*, the concentration dependence of D is eventually expected to become independent of molar mass, due to the transition of the relaxation mechanism from overall chain motion in the dilute solution to motions of strands the size of the screening length in the semidilute regime [13]. This merging of the diffusion coefficients is sketched in Fig. 1 with dotted lines.

The translational diffusion coefficients are shown together with data obtained from PCS, today's most widely employed experimental technique for diffusion coefficient measurements. In the hydrodynamic limit, characterized by $qR_g \ll 1$, where R_g is the single-chain radius of gyration, both techniques are expected to measure the same mutual diffusion coefficient [14]. Similar to the TDFRS diffusion coefficients, the PCS results are obtained as the first cumulants of the electric field autocorrelation function.

Before the data can be compared they need to be corrected for the different temperatures at which the experiments have been conducted (22°C for PCS and 24°C for TDFRS).

In the dilute regime, the mutual diffusion coefficient can be expressed in a virial expansion [15]:

$$D = \frac{kT}{f}(1-\phi)^2(1 + A_2 Mc + \cdots) \tag{14}$$

ϕ is the polymer volume fraction, A_2 the second virial coefficient, and f the friction coefficient of the polymer chain. For infinite dilution, f is given by the Stokes–Einstein relation,

$$f = 6\pi\eta_0 R_h \tag{15}$$

with η_0 being the solvent viscosity and R_h the single-chain hydrodynamic radius. For small temperature differences and low concentrations, the temperature dependence of A_2 is neglected, and the temperature dependence of f can be approximated by the Arrhenius-like thermal activation for the pure solvent viscosity: $\eta_0 \propto \exp(-E_a/kT)$, $E_a^{\text{toluene}} = 8820\ \text{J} \cdot \text{mol}^{-1}$ [5]. The temperature-corrected D values obtained from PCS agree nearly perfectly with the TDFRS data (Fig. 1).

4.2. Polydispersity

After closer examination, there is still a systematic deviation of the PCS diffusion coefficients toward smaller values. While this was not

understood at first [12], it is explained quantitatively by the not negligible —though small—polydispersity of the polystyrene calibration standards, together with the different statistical weights for different molar masses encountered in both experiments. The latter property can advantageously be exploited to obtain polydispersity information [16]. A detailed discussion is, however, beyond the scope of this paper.

Attention should be paid to the differences in the diffusion coefficients measured by TDFRS, as discussed in this paper, and the widely employed technique of "conventional" forced Rayleigh scattering [17] on polymer solutions and melts. There, photochemical labels are covalently attached to the polymer chains. Photobleaching of these labels creates an optical contrast, but the labeled and unlabeled chains are assumed to behave otherwise identical. After a grating has been written, it is blurred by the motion of the labels, reflecting the motion of the polymer chains. Since, from the viewpoint of the diffusing polymers, no concentration gradient with respect to the solvent is built up, the self-diffusion coefficient is measured by this technique [18].

4.3. Thermal Diffusion Coefficient and Soret Coefficient

The Soret coefficients as shown in Fig. 2 are determined from the fit of Eq. (10), and the thermal diffusion coefficients are computed from $D_T = S_T D$. This procedure is adequate for monodisperse systems that can be described by a single relaxation time. For polydisperse samples with a nonexponential time dependence, S_T is obtained from the saturation value and D_T from the initial slope of the concentration signal, according to Eq. (11). In either case the weight average of the respective quantity is measured. It can be shown that the determination of D_T from the initial slope of the heterodyne signal is very robust against perturbations, such as jitter of the grating or imperfect 180° phase jumps. Even in the presence of strong convective currents the correct thermal diffusion coefficient can be measured (but not the correct translational diffusion coefficient). For the weak polydispersities discussed here, either method yields the correct result.

As already known from the literature, D_T is, within experimental resolution, almost independent of molecular weight, and there is only a very weak concentration dependence. In the limit of infinite dilution, $D_T \approx (1.05 \pm 0.05) \times 10^{-7}\,\mathrm{cm^2 \cdot s^{-1} \cdot K^{-1}}$ is found. This value is very close to the zero-concentration result reported by Meyershoff and Nachtigall from measurements with a macroscopic thermal diffusion cell at 20°C [6]. They found, however, a decrease in D_T with increasing concentration, and at $c = 40$ g/l their value is only $0.86 \times 10^{-7}\,\mathrm{cm^2 \cdot s^{-1} \cdot K^{-1}}$, compared to $1.15 \times 10^{-7}\,\mathrm{cm^2 \cdot s^{-1} \cdot K^{-1}}$ found in this work. Giddings *et al.* [19]

employed thermal field flow fractionation (TFFF) and found values between 1.13 and $1.31 \times 10^{-7}\,cm^2 \cdot s^{-1} \cdot K^{-1}$ at temperatures between 23 and 29.5°C. TFFF results correspond effectively to zero concentration. The reasonable agreement among the three experimental methods suggests, at least for infinite dilution, a D_T slightly above $1.0 \times 10^{-7}\,cm^2 \cdot s^{-1} \cdot K^{-1}$. Up to now, polystyrene in toluene is the polymer/solvent system for which most experimental data are available. Whereas there is an acceptable agreement between the above authors, there are also diverging results in the literature, with deviations up to 400%. A more detailed discussion of these diverging results is given in Refs. 6 and 19.

Since D_T is nearly constant, the concentration and temperature dependence of S_T is governed mainly by the inverse translational diffusion coefficient (Fig. 2). Correspondingly, the Soret coefficient decreases with concentration—faster for higher molar masses. In the semidilute and concentrated regime, S_T is expected to become eventually molar mass independent, but the respective measurements still need to be done.

5. CONCLUSIONS

The translational and thermal diffusion coefficients and the Soret coefficients have been measured for polystyrene in toluene as a function of molar mass and concentration with the transient grating technique of TDFRS. While most measurements were conducted within the dilute regime, the technique is not limited to low concentrations. Excellent agreement with diffusion coefficients measured by photon-correlation spectroscopy has been found. Small differences, of the order of 1–2%, are due to the polydispersity of the samples. The molar mass independence of the thermal diffusion coefficient is confirmed within experimental resolution. In the limit of infinite dilution there is a reasonable agreement between the results from this work and those reported by Giddings et al. [19] and by Meyerhoff et al. [6], whereas results obtained by other authors deviate substantially. For higher concentrations, fewer data are available and the differences are more pronounced.

ACKNOWLEDGMENT

The authors thank the polymer analytical group of the institute for constant support, especially B. Müller for measuring the constrast factors.

REFERENCES

1. P. Debye and A. M. Bueche, in *High Polymer Physics*, H. A. Robinson, ed. (Chemical, Brooklyn, NY, 1948).

2. G. H. Langhammer, H. Pfennig, and K. Quitzsch, *Z. Elektrochem.* **62**:458 (1958).
3. K. Nachtigall and G. Meyerhoff, *Makromol. Chem.* **33**:85 (1959).
4. J. C. Giddings, *J. Chem. Phys.* **49**:81 (1968).
5. M. E. Schimpf and J. C. Giddings, *J. Polym. Sci.* **B27**:1317 (1989).
6. G. Meyerhoff and K. Nachtigall, *J. Polym. Sci.* **57**:227 (1962).
7. F. Bloisi, L. Vicari, P. Cavaliere, S. Martellucci, J. Quartieri, P. Mormile, and G. Pierattini, *Appl. Phys.* **B44**:103 (1987).
8. W. Köhler, *J. Chem. Phys.* **98**:660 (1993).
9. P. Kolodner, H. Williams, and C. Moe, *J. Chem. Phys.* **88**:6512 (1988).
10. H. J. V. Tyrrell, *Diffusion and Heat Flow in Liquids* (Butterworth, London, 1961).
11. H. J. Eichler, P. Guenther, and D. W. Pohl, *Laser-Induced Dynamic Gratings* (Springer, Berlin, 1986).
12. W. Köhler and P. Rossmanith, *Int. J. Polym. Anal. Character.* (in press).
13. E. J. Amis and C. C. Han, *Polymer* **23**:1403 (1982).
14. B. J. Berne and R. Pecora, *Dynamic Light Scattering* (Wiley, New York, 1976).
15. W. Brown (ed.), *Dynamic Light Scattering* (Clarendon Press, Oxford, 1993).
16. M. Corti, V. Degiorgio, M. Giglio, and A. Vendramini, *Opt. Commun.* **23**:282 (1977).
17. H. Hervet, W. Urbach, and F. Rondelez, *J. Chem. Phys.* **68**:2725 (1978).
18. H. Sillescu, *Makromol. Chem. Makromol. Symp.* **18**:135 (1988).
19. J. C. Giddings, K. D. Caldwell, and M. N. Myers, *Macromolecules* **9**:106 (1976).